

## Single Gap Transflective Liquid Crystal Display with Dual Orientation of Liquid Crystal

Young Jin LIM, Je Hoon SONG, Yong Bae KIM<sup>1</sup> and Seung Hee LEE\*

School of Advanced Materials Engineering, Chonbuk National University, Chonju-si, Chonbuk 561-756, Korea

<sup>1</sup>Liquid Crystal Research Center, Department of Chemistry, College of Sciences, Kon-Kuk University, 1, Hwayangdong, Kwangjinku, Seoul 143-701, Korea

(Received April 2, 2004; accepted May 23, 2004; published July 2, 2004)

We propose a single-cell-gap transflective liquid crystal display (LCD) with dual orientation of LC at an initial state. Owing to hybrid alignment in the reflective region, the effective cell retardation value becomes half of that in the transmissive region where the LCs are homogeneously aligned. Consequently, a transflective display driven by a vertical or fringe electric field with a single cell gap and high image quality is realized. [DOI: 10.1143/JJAP.43.L972]

KEYWORDS: single-gap transflective LCD, hybrid alignment, homogenous alignment

Recently, the role of transflective liquid crystal displays is becoming important because they can be used both outdoors and indoors with relatively lower power consumption than that of transmissive displays.<sup>1,2)</sup> Previous results from homogenous cells with a compensation film driven by a vertical electric field (named ECB),<sup>3–7)</sup> as well as a fringe electric field (named FFS)<sup>8,9)</sup> with dual-color-filter structures for dual-cell-gap and single-gap transflective displays using multidriving circuits,<sup>10)</sup> have been reported. For a transflective display with a multidriving circuit where the LCs are vertically aligned (VA) at the initial state, a single-cell-gap is used but the cost of circuit parts increases. In the dual-gap structure, the cell gap ( $d$ ) in the transmissive ( $T$ ) region is twice that in the reflective ( $R$ ) region since the optimal cell retardation values in the  $T$  and  $R$  regions should be half-wave plate ( $\lambda/2$ ) and quarter-wave plate ( $\lambda/4$ ), respectively, and thus the fabrication process is relatively complex compared with that of pure reflective or transmissive LCDs. Furthermore, the cell retardation value in the area between the  $T$  and  $R$  regions is between  $\lambda/2$  and  $\lambda/4$ , and, as such, it causes light leakage in the normally black (NB) mode and nonuniformity in image quality in the normally white (NW) mode. In addition, the ECB and VA cells show a very narrow viewing angle in the  $T$  region since the LC director tilts toward one direction causing a strong transmittance difference according to the viewing direction.

To solve the dual-gap and narrow viewing-angle problems, a new cell structure has been devised for the transflective display using a single cell gap which could be driven by either a vertical or fringe electric field, where the LC has a hybrid alignment in the  $R$  region and a homogenous alignment in the  $T$  region.<sup>11)</sup> The detailed electrooptic characteristics are described in each case.

Figure 1 shows LC alignment in the single-cell-gap transflective display. In the  $R$  region, the LC has a hybrid alignment while it has a homogenous alignment in the  $T$  region. The LC on the bottom substrate has homogeneous alignment in both regions while the LC has dual alignment on the top substrate. The homogenous alignment of the top substrate is made possible by exposing a vertical alignment using UV<sup>12)</sup> or ion beam<sup>13)</sup> into the transmissive area. However, in this study, the top substrate is covered by a homogenous alignment material at first and then after

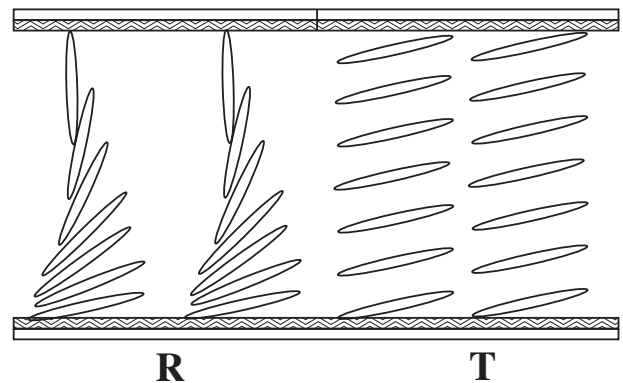


Fig. 1. LC orientation in the single gap transflective LCD.

blocking the  $T$  region with a protective film, the vertical alignment material is coated on a homogenous alignment material in the  $R$  region. As a result, the effective cell retardation value in the  $R$  region equals about half of the  $T$  region,<sup>11)</sup> i.e., when it is  $\lambda/2$  in the  $T$  region, it falls to  $\lambda/4$  in the  $R$  region. Owing to this, a single-gap transflective display is realized.

Figure 2 shows the optical cell configuration of single gap transflective displays using a vertical field and a fringe field. For a vertical field driven cell in the ECB mode, the NW

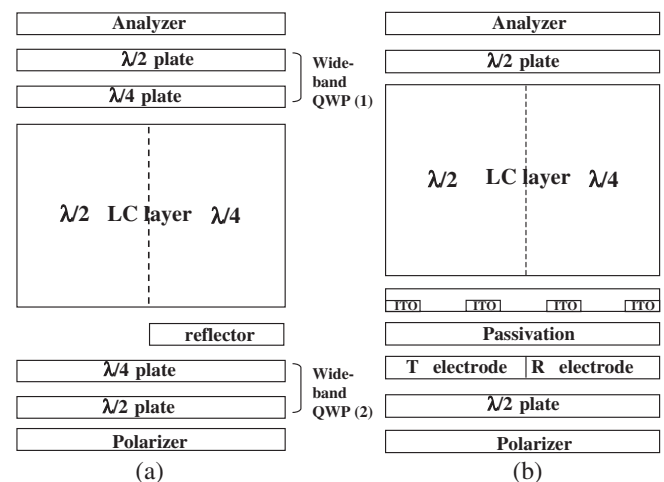


Fig. 2. Optical components of transflective TFT-LCD driven by (a) vertical field and (b) fringe field.

\*To whom correspondence should be addressed.  
 E-mail address: lsh1@moak.chonbuk.ac.kr

display was evaluated, whereas for a fringe-field-driven cell in the FFS mode, the NB cell was evaluated because the optic axis with a given retardation value rotates in plane according to bias, instead of a decrease in the retardation value such as in the ECB cell. For the FFS cell, compensation films of  $\lambda/2$  are inserted on the top and bottom of the LC layer, as shown in Fig. 2(b). In the device, the first electrode divides into the reflective and transparent regions and a transparent indium-tin-oxide (ITO) pixel electrode with a width of approximately  $3\mu\text{m}$  is located above the passivation layer with some distance.

To evaluate the electrooptic characteristics of the proposed device, calculations were performed on the transmittance and reflectance using the  $2 \times 2$  extended Jones matrix.<sup>14</sup> In the ECB cell, the LC with a birefringence ( $\Delta n$ ) of 0.089 and dielectric anisotropy ( $\Delta\epsilon$ ) of 7.4 was used and the cell gap ( $d$ ) was  $3.4\mu\text{m}$ . In the FFS cell, the LC with  $\Delta n$  of 0.070 and  $\Delta\epsilon$  of  $-4.0$  was used and the  $d$  was  $4\mu\text{m}$ . The pretilt angle of the bottom substrate was  $2^\circ$  in both the  $R$  and  $T$  regions, but on the top substrate, it was  $2^\circ$  and  $90^\circ$  in the  $T$  and  $R$  regions, respectively. The transmittance in the two parallel polarizers was assumed to be 0.35. Figure 3 shows detailed optical configurations of each layer in the ECB and FFS cells. In the ECB cell, the slow axes of each layer are the same as those described in the previous report except that the LC has a hybrid alignment in the  $R$  region.<sup>3</sup> In the FFS cell, in order to improve the viewing angle in the  $T$  region, the polarizer makes angles of  $75^\circ$  and  $15^\circ$  with the  $\lambda/2$  compensation film and the LC layer, respectively.<sup>15</sup> As such, the linearly polarized light vibrating at  $177^\circ$  in the  $T$  region propagates in the direction of  $87^\circ$  after passing through the film, the LC layer and the film again, and thus the cell appears to be black. With bias voltage, the LC rotates by  $45^\circ$  due to the fringe field and then a white state is obtained. Figure 4 shows voltage-dependent reflectance and transmittance curves in the ECB and FFS cells when the incident light is  $550\text{nm}$ . In the ECB cell, the light efficiency is very high but the driving voltage is also rather high since a high voltage is required to completely remove the residual phase. In addition, the  $R$  region has a lower threshold voltage than the  $T$  region, which may require dual driving circuits to generate the same grey level color chromaticity in the  $T$  and  $R$  regions. In the FFS cell, the  $R$  region has a slightly higher

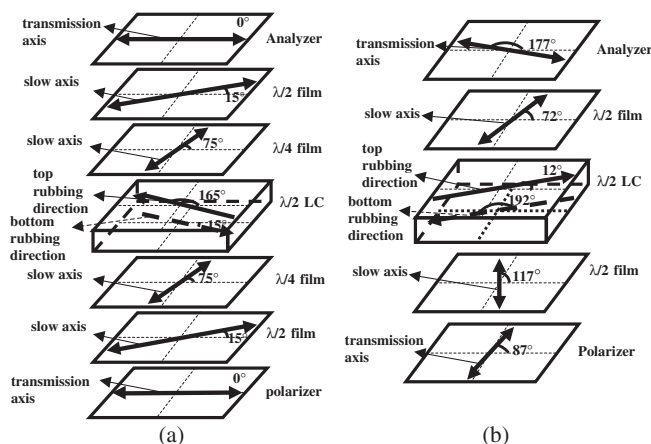


Fig. 3. Cell configuration of the single gap transfective LCDs used for simulation in the (a) ECB mode and (b) FFS mode.

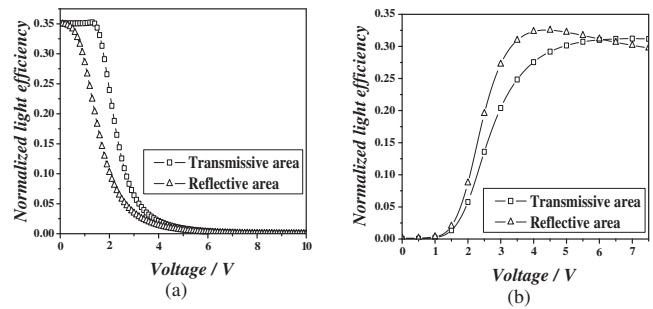


Fig. 4. Voltage-dependent light efficiency in the (a) ECB and (b) FFS cells when the wavelength of the incident light is  $550\text{nm}$ .

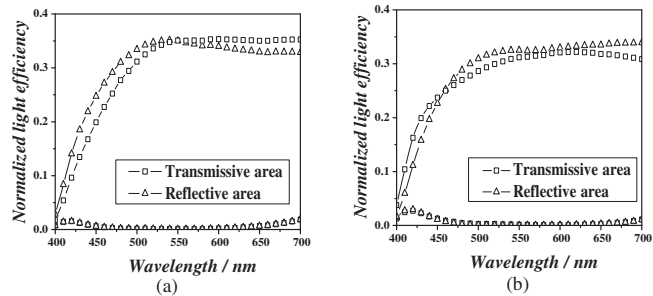


Fig. 5. Wavelength dependence of dark and white states of the  $T$  and  $R$  regions in the (a) ECB and (b) FFS cells.

light efficiency than that in the  $T$  region since the optimal cell retardation value for maximal light efficiency is slightly different in each region. Figure 5 shows the wavelength dispersion of the dark and white states in the ECB and FFS cells. In the ECB cell, the wavelength dispersion of the dark state in both the  $R$  and  $T$  regions was very small due to the use of a wide-band quarter-wave film (QWF). Even in the FFS cell, good wavelength characteristic is obtained. Figure 6 shows isocontrast curves in the  $T$  and  $R$  regions in each mode for an incident light of  $550\text{nm}$ . In the ECB cell, the region in which the contrast ratio is greater than 5 exists at a polar angle of more than  $40^\circ$  in all directions of the  $R$  region, but it is limited to  $40^\circ$  in the  $T$  region due to grey scale inversion. In the FFS cell, it exists at a polar angle of more than  $50^\circ$  in all directions in both the  $T$  and  $R$  regions with the absence of grey-scale inversion. From the results, one can conclude that the ECB cell has advantages in term of light efficiency while the FFS cell has strong merits in terms of the image quality.

Several test cells were fabricated to compare with calculated results. Here, the homogenous and vertical alignment materials, AL16139 and AL00010, respectively, from the Japan Synthetic rubber, were used. The physical properties of the superfluorinated LCs are the same as those used in the simulation. The cells which were manufactured by the above-mentioned method, have dual alignment and they were observed under a polarizing microscope. Figure 7 shows optical photomicrographs of the dark and white states in the ECB and FFS cells, respectively. In the ECB and FFS cells, the transmitted light shows different intensities in the  $R$  and  $T$  regions, which indicates that the cell retardation values in the  $T$  and  $R$  regions are different from each other. Furthermore, a good dark state is observed without showing

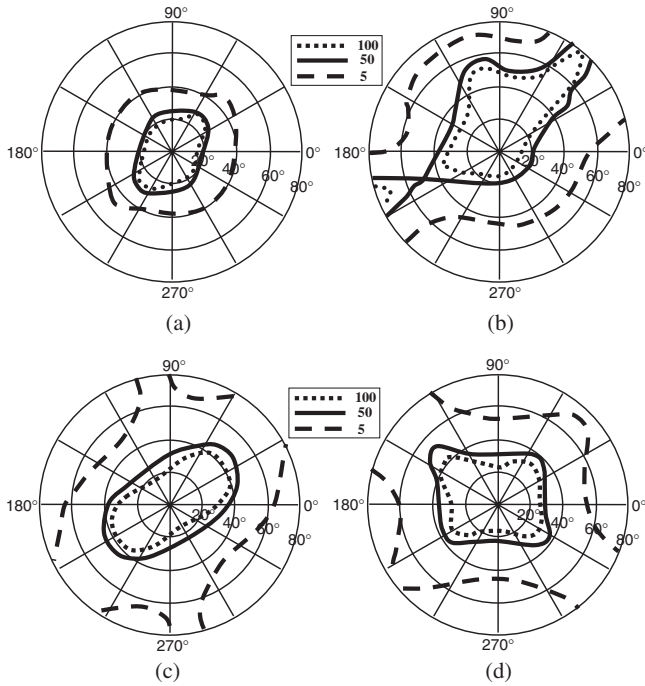


Fig. 6. Isocontrast contour at an incident wavelength of 550 nm for the transmissive region in (a) ECB and (c) FFS cells and that for the reflective region in the (b) ECB and (d) FFS cells.

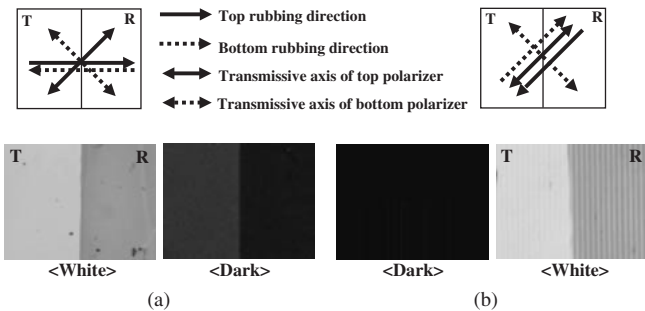


Fig. 7. Optical photomicrographs of dark and white states of the *T* and *R* regions in the (a) ECB and (b) FFS cells.

any disclination lines between domains because the LC director tilts toward the same direction along the vertical field in the ECB cell and rotates in the same direction along the fringe electric field in the FFS cell in the *R* and *T* regions, even though the LC has dual orientation. Figure 8 shows voltage-dependent transmittance and reflectance curves in the ECB and FFS cells. Both results show very similar curves with calculated results. As expected, the ECB cell shows a better light efficiency than the FFS cell while the driving voltage in the FFS cell is slightly lower than that in the ECB cell.

In summary, a single-gap transflective display with dual orientation, in which the LC has a hybrid alignment in the *R* region and a homogenous alignment in the *T* region, is proposed. Through this dual orientation, the cell retardation value may be as high as  $0.28 \mu\text{m}$ , allowing the transflective

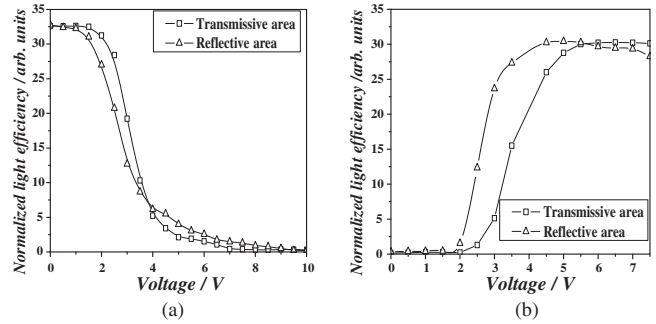


Fig. 8. Measured voltage-dependent transmittance and reflectance curves in the (a) ECB and (b) FFS cells when the wavelength of the incident light is 550 nm.

display to have a high single cell gap. The device driven by a fringe electric field particularly produces a high image quality in both the reflective and transmissive regions with a slight loss of light efficiency. This new device has the potential to become an integral part of transflective displays.

This work was performed by the Advanced Backbone IT technology development project supported by the Ministry of Information & Communication in Republic of Korea.

- 1) E. Yoda, T. Uesaka, T. Ogasawara and T. Toyooka: Dig. Technical Paper SID, Society for Information Display, Boston, 2002, p. 762.
- 2) R. Watanabe and O. Tomita: *Proc. 9th Int. Display Workshops* (Society for Information Display and The Institute of Image Information and Television Engineers, Hiroshima, 2002) p. 397.
- 3) H-I. Baek, Y-B. Kim, K-S. Ha, D-G. Kim and S-B. Kwon: *Proc. 7th Int. Display Workshops* (Society for Information Display and The Institute of Image Information and Television Engineers, Kobe, 2000) p. 41.
- 4) T. Uesaka, E. Yoda, T. Ogasawara and T. Toyooka: *Proc. 9th Int. Display Workshops* (Society for Information Display and The Institute of Image Information and Television Engineers, Hiroshima, 2002) p. 417.
- 5) K. Fujimori, Y. Narutaki, Y. Itoh, N. Kimura, S. Mizushima, Y. Ishii and M. Hijikigawa: Dig. Technical Paper SID, Society for Information Display, Boston, 2002, p. 1382.
- 6) Y. Narutaki, K. Fujimori, Y. Itoh, T. Shinomiya, N. Kimura, S. Mizushima and M. Hijikigawa: *Proc. 9th Int. Display Workshops* (Society for Information Display and The Institute of Image Information and Television Engineers, Hiroshima, 2002) p. 299.
- 7) K-J. Kim, J. S. Lim, T. Y. Jung, C. Nam and B. C. Ahn: *Proc. 9th Int. Display Workshops* (Society for Information Display and The Institute of Image Information and Television Engineers, Hiroshima, 2002) p. 433.
- 8) S. H. Lee, S. L. Lee and H. Y. Kim: *Appl. Phys. Lett.* **73** (1998) 2881.
- 9) T. B. Jung, J. C. Kim and S. H. Lee: *Jpn. J. Appl. Phys.* **42** (2003) L464.
- 10) J. C. Kim, C. G. Jhun, K. H. Park, J. S. Gwag, S. H. Lee, G. D. Lee and T. H. Yoon: *Proc. 3rd IMID* (The Korean Information Display Society, Daegu, 2003) p. 283.
- 11) T. B. Jung, Y. J. Lim and S. H. Lee: *Proc. KJI* (Korean Society for Imaging Science Technology, Pusan, 2003) p. 15.
- 12) M. Schadt, H. Seiberle, A. Schuster and S. M. Kelly: *Jpn. J. Appl. Phys.* **34** (1995) L764.
- 13) S. H. Lee, K. H. Park, J. S. Gwag, T. H. Yoon and J. C. Kim: *Jpn. J. Appl. Phys.* **42** (2003) L5127.
- 14) A. Lien: *Appl. Phys. Lett.* **57** (1990) 2767.
- 15) S. H. Lee *et al.*: submitted to *Jpn. J. Appl. Phys.* (2004).